2

UCRL- 83057
PREPRINT
CONF-791135--2

EXPERIMENTS WITH POLYMER COATED MICROSPHERES IRRADIATED BY THE SHIVA LASER SYSTEM

J.M.Auerbach, K.R.Manes, D.L. Matthews,
L.N.Koppel, S.M.Lane, E.M. Campbell, N.Ceglio,
D.Phillion, P.H.Y.Lee, V.Rupert, D.Banner,
C.Swift, C.Hatcher, W.Mead

This paper was prepared for submittal to
the American Physical Society
Division of Plasma Physics
Boston, Mass.
November 12-16, 1979

November 10, 1979

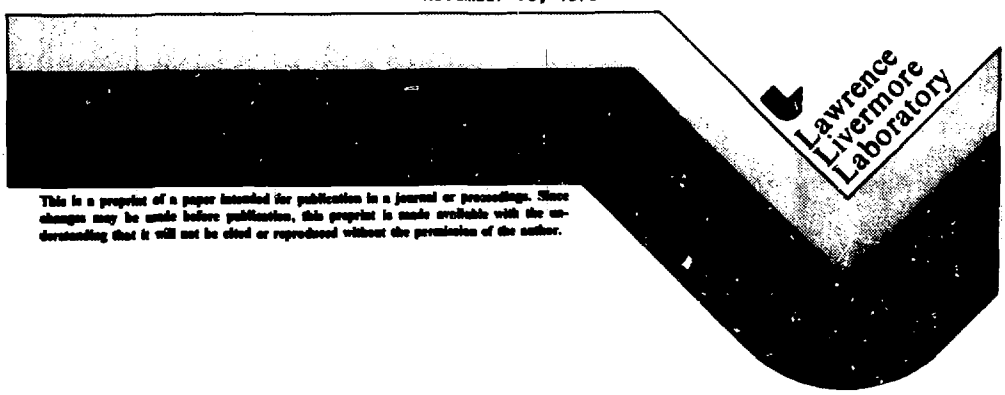

Experiments with Polymer Coated Microspheres Irradiated by the Shiva Laser System*

J. M. Auerbach, K. R. Manes, D. L. Matthews, L. N. Koppel, S. M. Lane, E. M. Campbell, N. M. Ceglio, D. W. Phillion, P. H. Y. Lee, V. C. Rupert, D. L. Banner, C. D. Swift, C. W. Hatcher, and W. C. Mead

University of California, Lawrence Livermore Laboratory
Livermore, California 94550

ABSTRACT

Polymer coated spherical targets have been irradiated by the Shiva laser system in an effort to compress the contained 10 mg/cc DT fuel to super liquid densities. Glass microspheres of 140 μm I.D. and 5 μm wall thickness with polymer coatings 15 μm - 100 μm thick have been irradiated with laser pulses of 4 kilojoules in 200 psec FWHM. Target performance was diagnosed with neutron yield measurements, radiochemistry, Argon line imaging, and x-ray imaging techniques. Ball in plate targets achieved greater implosion symmetry than free-standing ball targets. With yields of 10^7 - 10^3 neutrons, targets reached DT fuel compressions of several times liquid density.

*Work performed under the auspices of the U. S. Department of Energy by the Lawrence Livermore Laboratory under Contract No. W-7405-ENG-48.

The present effort of laser fusion research is towards the attainment of isentropic compression of DT fuel by ablative driven implosions. This is a far different operating regime than the exploding pusher target mode in which past experiments[2,3] produced high ion temperatures and high neutron yields but DT densities only a small fraction of liquid value (.2 g/cm^3). The ablative implosion is characterized by small shock preheat and smooth acceleration of the pusher whereas the exploding pusher is characterized by high preheat, decompression of the shell, and shock heating of the fuel.

The experiments described in this paper represent progress towards using ablation to compress DT fuel to super liquid densities. The compression is not isentropic as preheat of the pusher and fuel was found to exist. However, as will be shown below ablation had a significant role in the implosion process. The targets used were polymer coated glass microsphere filled with 10 mg/cm^3 of DT fuel and 0.1 atm of Argon. The microspheres had nominal inner diameters of 140 μm and nominal wall thicknesses of 5 μm. Nominal thickness of the $CF_{1.4}$ polymer ablators were 15 μm. Figure 1 shows the calculated time history of the ablator, pusher and fuel dynamics for a typical "140 X 5 + 15 CF" target. Details of the hydrodynamic code calculations will be presented in the paper by Mead[4] et. al. The principal characteristics to be noted are the ablation of the $CF_{1.4}$ ablator at 0.2 nsec - 0.3 nsec while the glass pusher remains essentially stationary followed by the inward acceleration and decompression of the pusher. The decompression of the pusher indicates this experiment is still far removed from the isentropic ablation-driven implosion. Calculated fuel density is ten times the liquid value, and calculated neutron yield is between 10^8 and 10^9, for absorption values between 15% and 30%. The calculated fuel density is almost constant in this range of absorption fraction.

Diagnostics used in the experiment monitored the performance of fuel and pusher laser, and plasma calorimeters measured the absorption of the targets which had a mean value of 20% to 5%. Neutron yield was measured by lead and copper activation detectors. The spectrum of the high energy x-rays was monitored by the filter fluorescer system. The implosion symmetry of the pusher was monitored by observing the emission of x-rays

from the glass with Kirkpatrick-Baez x-ray microscopes and x-ray zone plates. Radiochemistry and Argon line imaging were used to determine fuel density. These last two diagnostics will be discussed in detail in the paper by Campbell[5] et. al.

The targets used for the density measurements were 140 X 5 + 15 CF balls mounted on a stalk. The SHIVA beams were aligned "tangentially" to the surface of the ball as shown in Figure 2. The beam configuration of the SHIVA laser even with this alignment produced polar heating asymmetry as shown in the adjacent x-ray micrograph showing the 2 keV x-ray emission of the glass pusher. Figure 3 shows contour plots of this emission indicating a 2:1 asymmetry in the pusher implosion. The 1 keV channel image shows the hotter polar regions.

An improvement in implosion symmetry was achieved with a 140 X 5 + 15 CF ball in a CH plate irradiated as shown in Figure 4. For each SHIVA beam cluster one beam was directed at the pole of the ball and the other nine focused tightly at the equator. This resulted in a more uniform illumination as confirmed by the spherical implosion of the pusher as shown in the accompanying 2 keV x-ray micrograph. Shown in Figure 5 are the X, Y profiles of this implosion region indicating a spherical implosion. The upper micrograph shows the image on the 1 keV channel of the x-ray microscope. Note the absence of localized polar heating and the resulting uniform heating of the ball. This target, however; presented problems with the radiochemistry diagnostic and was not pursued further. Another disadvantage is that the plate diverts energy that could be utilized in heating the ball.

Figure 6 shows the performance of the 140 X 5 + 15 CF ball on stalk targets in terms of neutron yield vs incident joules/ng. In agreement with calculation, there is an increase in yield with incident joules/ng. Deviation from the correlation curve can be due to a number of factors such as beam imbalance, fluid instabilities and subsequent mixing of fuel and pusher.

Density measurement of the DT fuel posed the most formidable problem in the experiment. Two methods were used and the results will be emphasized in this paper. Details of the method will be discussed in the talk by Campbell[5] et. al. and are described in a paper by Koppel[6] et. al.

The primary density diagnostic was the radiochemistry or neutron activation technique which infers $\rho\Delta R$ of the compressed glass pusher by measurement of the number of activated Al^{28} atoms activated by the 14 MeV neutrons which interact with the Si atoms in the glass pusher. The relationship between $\rho\Delta R$ and ρ fuel is complex and non unique. In this paper we present two relationships

(1) Based on computer simulations of the 140 X 5 + 15 CF target

(2) A simple isobaric isothermal model which allows an analytic relationship between pusher $\rho\Delta R$ and fuel ρ provided one assumes a spherical implosion and uniform temperature and pressure in pusher and fuel. Due to the large errors in the calculations and experimental measurements one will see that very precise density measurements are unattainable at this time.

Computer calculations were based on experimental laser parameters (energy, pulse width, and absorption fraction and experimental x-ray spectra. Two limiting cases in 1-D were considered the case of "NO MIX" of pusher and fuel and "FULL MIX" of pusher and fuel. The derived relationships are shown in Figure 7. Three of the experiments yielded well defined values of pusher $\rho\Delta R$. These are shown on the plot to indicate the range of inferred density values. Note that these densities are based on a spherical implosion and that an ellipsoidal fuel region would lead to lower density values as well as require a time-consuming 2D or 3D calculation.

The principal steps in the derivation of the simple model relating pusher $\rho\Delta R$ and fuel density is shown in Figure 8. The equations can be similarly derived for an ellipsoidal compression provided the pusher and fuel have similar eccentricities. Since this condition cannot be verified experimentally one must put high errors on this analysis too. Later the values of density based on a spherical implosion and an ellipsoidal implosion with the 2:1 eccentricity of the region of Figure 2 will be presented.

Argon line imaging was used to infer density from 4 of the 140 X 5 + 15 CF ball experiments. Details of the imaging method which uses a small crystal spectrometer with a slit are presented in the report by Koppel[7] et. al. The spectrometer is oriented perpendicular to the beam direction

so only 1-dimensional information is obtained on a possible 3-dimensional imploded region. Hence additional information such as the x-ray images of the pusher region (Figures 1-4) can be used to infer the size of the compressed fuel core. Figure 9 shows one of the profiles of the helium-like line of Ar^{+16} (3-14 Kev) obtained on one of the experiments. Note that there is a moderate noise/signal level which was attributed primarily to the low pressure (0.1 atm) of the Argon seed gas in the fuel. Precise unfolding of the line profile is very difficult requiring knowledge of the opacity, shape of the imploded region, temperature distribution of the fuel, etc. The width of the Argon line film record was unfolded to give a core dimension imaged by the slit for the case of a spherical implosion and an oblate implosion of 2:1 eccentricity based on the x-ray microscope data. The results are shown in Figure 10, summarized along with the radiochemistry results. In general, the computer simulation results infer higher fuel densities than the simple model or Argon line results. Nevertheless, the results are consistent within the error range and imply fuel densities of several times liquid value have been reached.

REFERENCES

1. J. Nuckolls, L. Wood, A. Thiessen, and G. Zimmerman, Nature (London) 239, 139 (1972)

2. E. K. Storm, et. al. Phys. Rev. Lett. 40, 1578 (1978)

3. D. R. Speck, et. al. Lawrence Livermore Laboratory Report UCRL 82117, June, 1979

4. W. C. Mead, et. al. Lawrence Livermore Laboratory Report UCRL 83163, October, 1979

5. E. M. Campbell, et. al. Lawrence Livermore Laboratory Report UCRL 83275, November, 1979

6. L. N. Koppel, et. al. Lawrence Livermore Laboratory Report UCRL 83313, September, 1979

LIST OF FIGURES

RADIUS VERSES TIME FOR "10X" BALL TARGET SHOWS EARLY ABLATION FOLLOWED BY PUSHER DECOMPRESSION

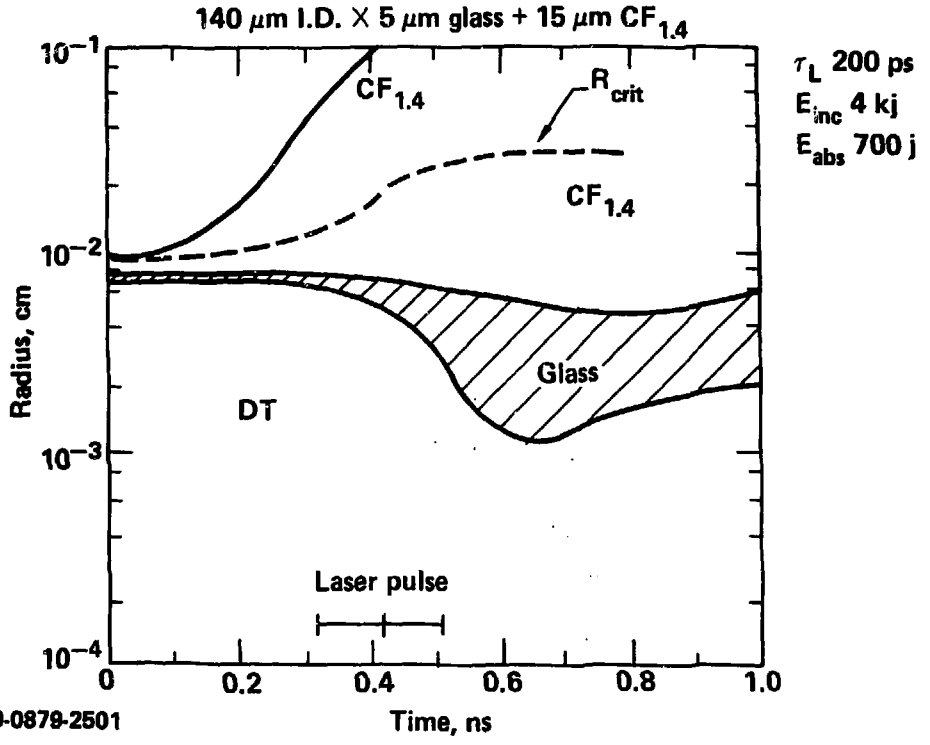

Figure 1

BALL-ON-STALK IRRADIATION GEOMETRY

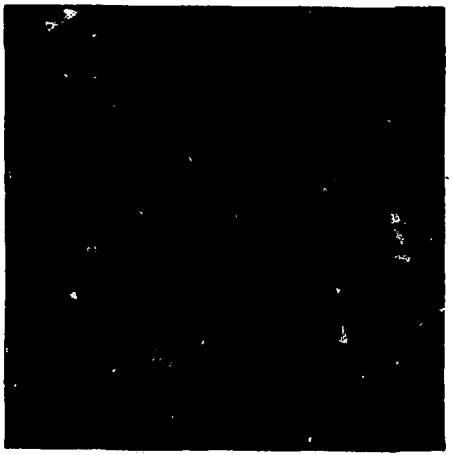

X-ray micrograph

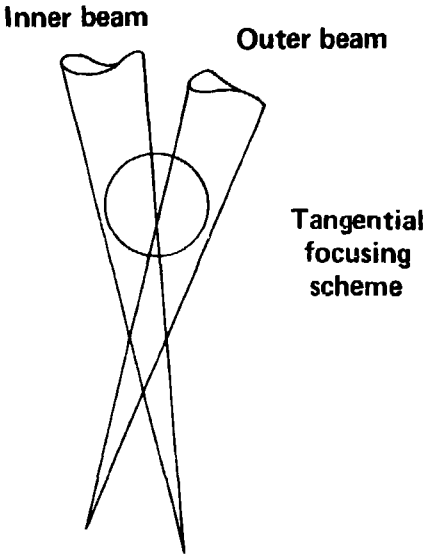

20-50-0979-2503

Figure 2

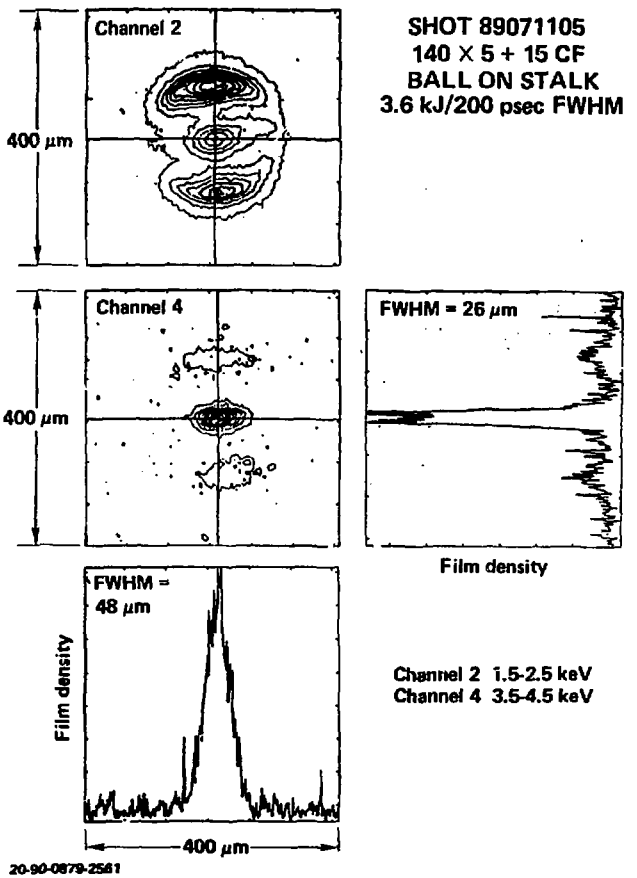
Channel 2
400 μm
SHOT 89071105
140 X 5 + 15 CF
BALL ON STALK
3.6 kJ/200 psec FWHM
Channel 4
400 μm
FWHM = 26 μm
Film density
FWHM =
48 μm
Film density
Channel 2 1.5-2.5 keV
Channel 4 3.5-4.5 keV
400 μm
20-90-0879-2561

Figure 3

BALL-IN-PLATE IRRADIATION GEOMETRY

X-ray micrograph

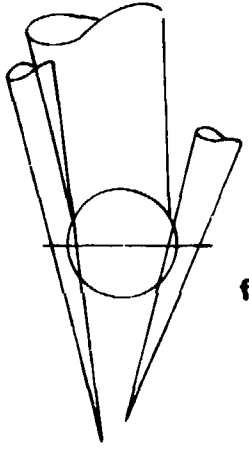

9 around 1
focusing scheme

28-80-0879-2804

Figure 4

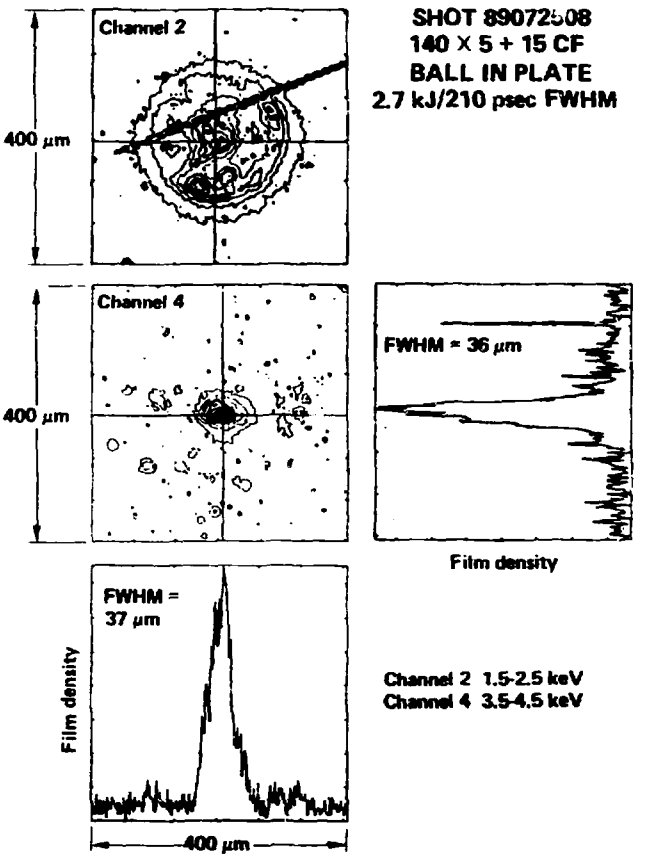
Channel 2
400 μm
SHOT 89072508
140 X 5 + 15 CF
BALL IN PLATE
2.7 kJ/210 psec FWHM
Channel 4
400 μm
FWHM = 36 μm
Film density
FWHM =
37 μm
Film density
Channel 2 1.5-2.5 keV
Channel 4 3.5-4.5 keV
400 μm

Figure 5

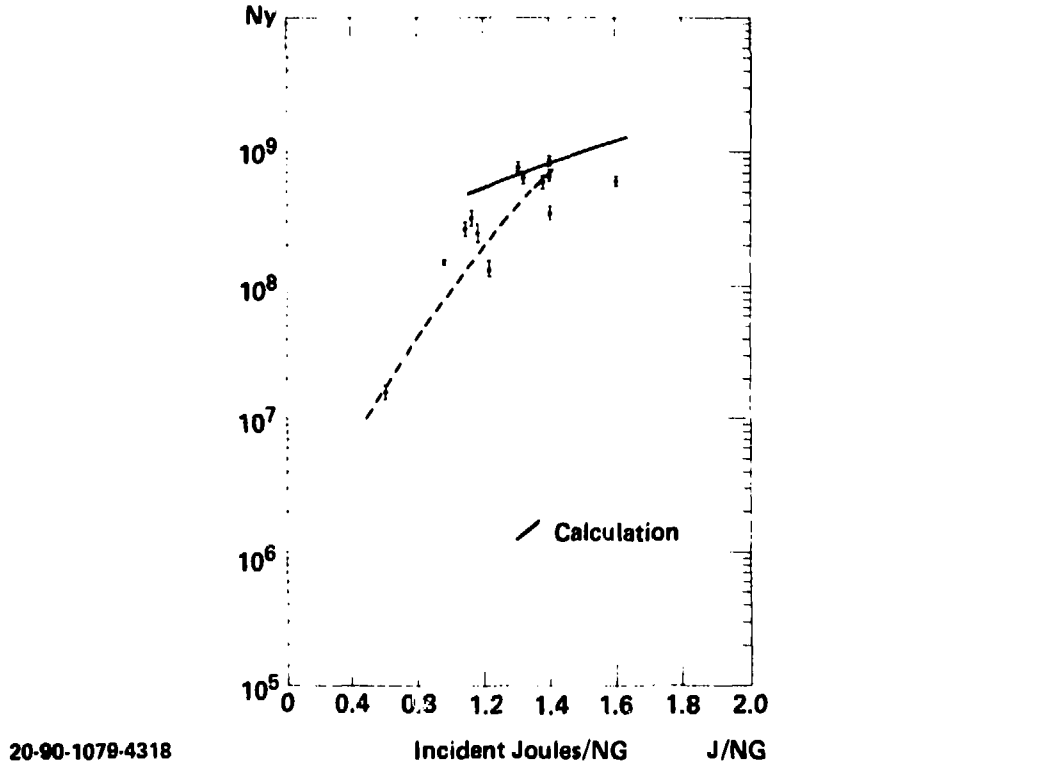
140 X 5 + 15 CF BALL YIELD VS JOULES/NG
Ny
10^9
10^8
10^7
10^6
10^5
0
0.4
0.8
1.2
1.4
1.6
1.8
2.0
Calculation
20-90-1079-4318
Incident Joules/NG
J/NG

Figure 6

FUEL DENSITY FROM RADIO CHEMISTRY

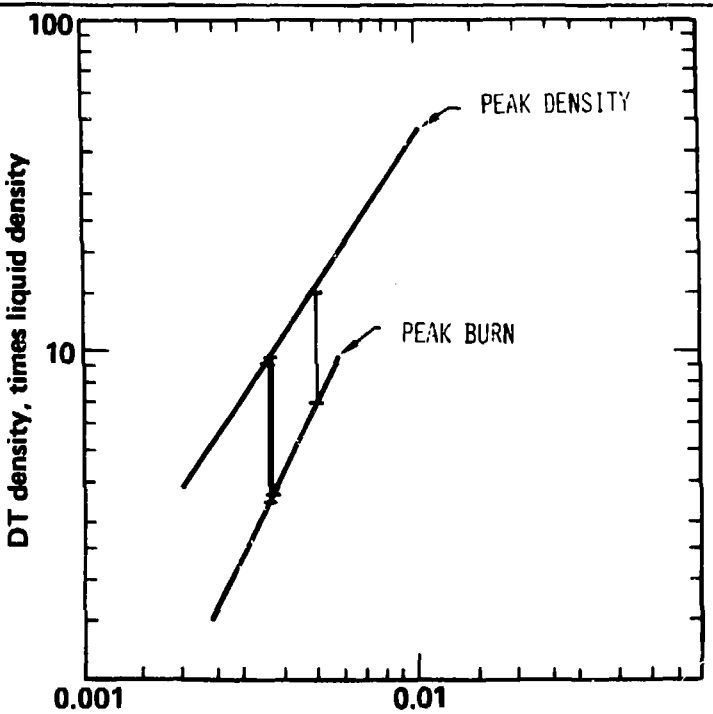

20-90-0879-2502

Figure 7

PUSHER $\rho\Delta r$ IS RELATED TO FUEL DENSITY

$$\frac{\frac{4}{3}\pi r_f^3(f)\rho_f(f)}{\frac{4}{3}\pi\left[r_f^3(p) - r_f^3(f)\right]\rho_f(p)} = \frac{M_f(f)}{M_f(p)} = \frac{M_0(f)}{M_0(p)} = \frac{\frac{4}{3}\pi r_0^3(f)\rho_0(f)}{4\pi r_0^2(f)\rho_0(p)\Delta r_0}$$

$$\frac{r_f(f)\rho_f(f)}{\Delta r_f\left[3 + 2\frac{\Delta r_f}{r_f(f)} + \left(\frac{\Delta r_f}{r_f(f)}\right)^2\right]\rho_f(p)} = \frac{r_0(f)\rho_0(f)}{3\rho_0(p)\Delta r_0}$$

$$\frac{r_f(f)\rho_f(f)}{r_0(f)\rho_0(f)} = \frac{\rho_f(p)\Delta r_f}{\rho_0(p)\Delta r_0}\left[1 + \frac{2}{3}\frac{\Delta r_f}{r_f(f)} + \frac{1}{3}\left(\frac{\Delta r_f}{r_f(f)}\right)^2\right]$$

$$\rho_f(f) = \rho_0(f)\left\{\frac{\rho_f(p)\Delta r_f}{\rho_0(p)\Delta r_0}\left[1 + \frac{2}{3}\frac{\Delta r_f}{r_f(f)} + \frac{1}{3}\left(\frac{\Delta r_f}{r_f(f)}\right)^2\right]\right\}^{3/2}$$

20-90-0479-1083

Figure 8

ARGON LINE IMAGING CRYSTAL SPECTROMETER RECORDS OF THE IMPLODED PLASMA

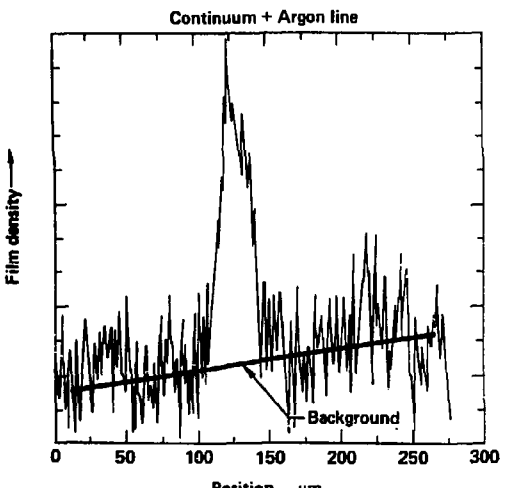

~22 μm source size for Argon line + continuum

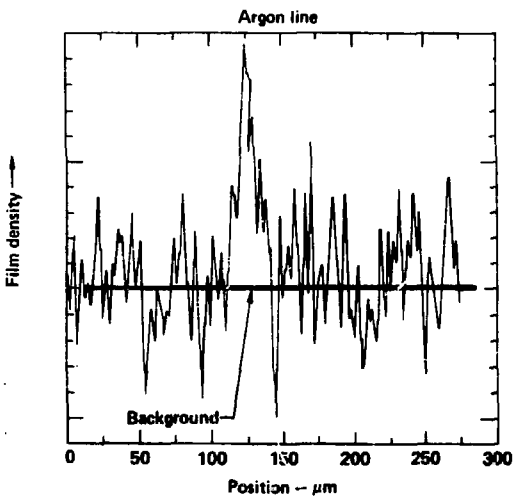

~20 μm source size for Helium like Argon line, Ar^{+16}, at 3.14 KeV

20-80-0879-2559

Figure 9

140 X 5 + 15 CF BALL EXPERIMENTS DENSITY MEASUREMENTS

Shot no.	Neutron yield	Pusher	X liquid density			X liquid density	
		ρR_{eff} (G/cm^2)	ρ_{DT} (Simple model)	ρ_{DT} (Simulation results)	Argon line	ρ_{DT} (Argon line imaging)	
						Sphere	2:1 ellipsoid
89071705	$(1.56 \pm 0.22) \times 10^7$				√	5 ± 2	1.3 ± 0.5
89072310	$(6.7 \pm 0.6) \times 10^6$	0.0059 ± 0.0015	$5.2^{+2.1}_{-1.9}$	NM 18^{+8}_{-7} FM $9^{+4}_{-4.6}$			
89072513	$(1.30 \pm 0.14) \times 10^8$	0.0047 ± 0.0022	$3.7^{+1.9}_{-2.3}$	NM $13^{+10}_{-7.3}$ FM $5.6^{+6.4}_{-3.9}$		23 ± 9	$6^{+3}_{-2.5}$
89073104	$(6.5 \pm 0.7) \times 10^8$				√	5 ± 2	1.3 ± 0.4
89073106	$(3.5 \pm 0.4) \times 10^8$	0.0063 ± 0.0018	$5.7^{+2.5}_{-2.2}$	NM 19^{+11}_{-6} FM $10.5^{+7.5}_{-5.3}$	√	5 ± 2	1.3 ± 0.4

NM = no mix
FM = full mix

Figure 10